

Article

# Electron-Deficient Ru(II) Complexes as Catalyst Precursors for Ethylene Hydrophenylation

Xiaofan Jia , Songyuan Tian, Philip J. Shivokevich, W. Dean Harman, Diane A. Dickie  and T. Brent Gunnoe \*

Department of Chemistry, University of Virginia, Charlottesville, VA 22904, USA; xiaofan.jia@yale.edu (X.J.); sst2nh@virginia.edu (S.T.); pjs6kb@virginia.edu (P.J.S.); wdh5z@virginia.edu (W.D.H.); dad8v@virginia.edu (D.A.D.)

\* Correspondence: tbg7h@virginia.edu

**Abstract:** Ruthenium(II) complexes with the general formula  $\text{TpRu(L)(NCMe)Ph}$  ( $\text{Tp}$  = hydrido(trispyrazolyl)borate,  $\text{L}$  = CO,  $\text{PMe}_3$ ,  $\text{P(OCH}_2)_3\text{CEt}$ ,  $\text{P(py)}_3$ ,  $\text{P(OCH}_2)_2(\text{O)CCH}_3$ ) have previously been shown to catalyze arene alkylation via Ru-mediated arene C–H activation including the conversion of benzene and ethylene to ethylbenzene. Previous studies have suggested that the catalytic performance of these  $\text{TpRu(II)}$  catalysts increases with reduced electron-density at the Ru center. Herein, three new structurally related Ru(II) complexes are synthesized, characterized, and studied for possible catalytic benzene ethylation.  $\text{TpRu(NO)Ph}_2$  exhibited low stability due to the facile elimination of biphenyl. The Ru(II) complex  $(\text{Tp}^{\text{Br}_3})\text{Ru(NCMe)(P(OCH}_2)_3\text{CEt)Ph}$  ( $\text{Tp}^{\text{Br}_3}$  = hydridotris(3,4,5-tribromopyrazol-1-yl)borate) showed no catalytic activity for the conversion of benzene and ethylene to ethylbenzene, likely due to the steric bulk introduced by the bromine substituents.  $(\text{Ttz})\text{Ru(NCMe)(P(OCH}_2)_3\text{CEt)Ph}$  ( $\text{Ttz}$  = hydridotris(1,2,4-triazol-1-yl)borate) catalyzed approximately 150 turnover numbers (TONs) of ethylbenzene at 120 °C in the presence of Lewis acid additives. Here, we compare the activity and features of catalysis using  $(\text{Ttz})\text{Ru(NCMe)(P(OCH}_2)_3\text{CEt)Ph}$  to previously reported catalysis based on  $\text{TpRu(L)(NCMe)Ph}$  catalyst precursors.

**Keywords:** olefin hydroarylation; ruthenium; catalysis; ethylbenzene; C–H activation



**Citation:** Jia, X.; Tian, S.; Shivokevich, P.J.; Harman, W.D.; Dickie, D.A.; Gunnoe, T.B. Electron-Deficient Ru(II) Complexes as Catalyst Precursors for Ethylene Hydrophenylation. *Inorganics* **2022**, *10*, 76. <https://doi.org/10.3390/inorganics10060076>

Academic Editors: Wolfgang Linert, Duncan H. Gregory, Richard Dronskowski, Vladimir Arion, Claudio Pettinari and Torben R. Jensen

Received: 10 May 2022

Accepted: 27 May 2022

Published: 31 May 2022

**Publisher's Note:** MDPI stays neutral with regard to jurisdictional claims in published maps and institutional affiliations.



**Copyright:** © 2022 by the authors. Licensee MDPI, Basel, Switzerland. This article is an open access article distributed under the terms and conditions of the Creative Commons Attribution (CC BY) license (<https://creativecommons.org/licenses/by/4.0/>).

## 1. Introduction

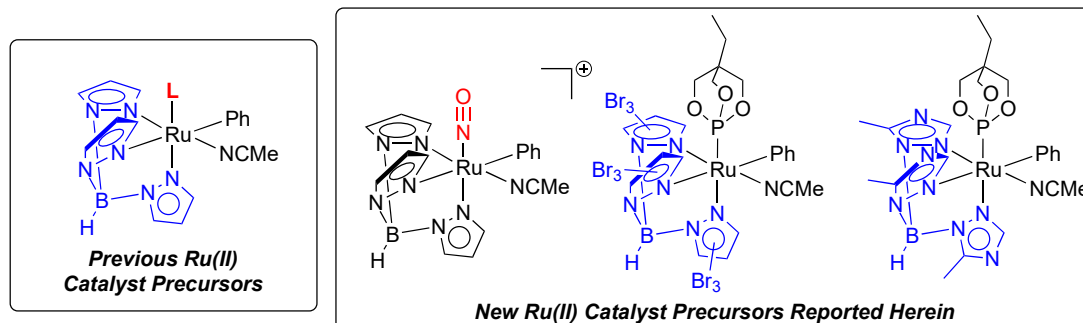
Alkyl arenes serve as precursors for a wide range of products, including polymers, pharmaceuticals, and surfactants. For example, ethylbenzene is produced on a scale of approximately 40 million tons each year [1]. The current industrial synthesis of alkyl arenes is accomplished either by a traditional Friedel–Crafts alkylation, which is catalyzed by a Lewis acid (e.g.,  $\text{AlCl}_3$ ) in the presence of a Brønsted acid (e.g., HF), or by using an acidic zeolite catalyst [2–6]. Due to the nature of the acid-mediated electrophilic arene substitution reaction, important reaction outcomes are dictated by the mechanism of the reaction. For example, the alkyl arene product is generally more reactive than the arene substrate, which can result in polyalkylation at even low or modest conversions [3]. Moreover, reactions using  $\alpha$ -olefins exclusively give products with  $x$ -aryl alkanes where  $x \geq 2$ . The selective synthesis of 1-aryl alkanes is not viable with current commercial catalytic processes for arene alkylation [7–10].

Catalytic arene alkylation has been reported using molecular complexes and homogeneous catalysts based on iridium [11,12], platinum [13–19], and ruthenium [20–28], and direct arene alkenylation has been reported using rhodium [29–39], ruthenium [40,41], and palladium [42,43] catalysts. These catalytic processes provide routes for the synthesis of alkyl and alkenyl arenes that provide complementary selectivity to acid-catalyzed arene alkylation reactions [3]. Recent success for Rh-catalyzed arene alkenylation to give anti-Markovnikov products and the newly reported Ni catalysis by the Hartwig and Eisenstein groups for the formation of 1-aryl alkanes or alkenes, which we have termed super linear

alkyl benzenes to differentiate from linear alkyl benzenes that are linear alkanes with internal phenyl substitution, suggest significant opportunities for new selectivity using molecular transition metal-based catalysts [7,9,10,37,44].

We have reported a series of studies on arene alkylation using Ru(II) catalyst precursors with the general formula  $\text{TpRu(L)(NCMe)Ph}$  ( $\text{L} = \text{CO}, \text{PMe}_3, \text{P}(\text{OCH}_2)_3\text{CEt}, \text{P}(\text{pyr})_3$  or  $\text{P}(\text{OCH}_2)_2(\text{O})\text{CCH}_3$ ;  $\text{Tp} = \text{hydridotr}(\text{pyrazolyl})\text{borate}$ ) including the catalytic conversion of ethylene and benzene to ethylbenzene. In these studies, we have discovered that the electron density of the Ru center has a significant influence on the catalyst performance and, in particular, catalyst longevity [25]. We have demonstrated that more strongly electron-withdrawing ligands  $\text{L}$  (e.g.,  $\text{L} = \text{CO}$ ) for catalyst precursors of the type  $\text{TpRu(L)(NCMe)Ph}$  increase catalyst longevity. Moreover, we have demonstrated that a cationic Ru(II) complex gives an increase in turnover number compared to catalysis with a closely related charge neutral Ru(II) catalyst precursor [21].

We sought to probe additional improvements in Ru catalyzed arene alkylation by introducing new ligands that reduced Ru-centered electron density (Scheme 1). Previously, our group determined and compared the electron density of the Ru(II) center using Ru(III/II) redox potentials from cyclic voltammetry [23–25]. A variety of ligands, including carbon monoxide, phosphines ( $\text{PMe}_3, \text{P}(\text{Pyr})_3$  where  $\text{Pyr} = \text{N-pyrrolyl}$ ), and phosphites ( $\text{P}(\text{OCH}_2)_3\text{CEt}, \text{P}(\text{OCH}_2)_2(\text{O})\text{CCH}_3$ ) with varying steric and electronic structures were installed as the  $\text{L}$  ligand on catalyst precursors of the type  $\text{TpRu(L)(NCMe)Ph}$  [26]. The most electron-poor complex among the series,  $\text{TpRu(CO)(NCMe)Ph}$ , proved to be the longest-lived catalyst [27]. The linear nitrosyl ligand, formally  $\text{NO}^+$ , is an analog of  $\text{CO}$  that is generally considered to be a stronger  $\pi$ -acceptor than  $\text{CO}$ . Thus, we considered that the cationic complex  $[\text{TpRu(NO)(NCMe)Ph}]^+$  would have a more electron-deficient Ru(II) center than  $\text{TpRu(CO)(NCMe)Ph}$ , and may potentially lead to enhanced catalytic performance.



**Scheme 1.** New Ru(II) complexes with reduced electron density compared to  $\text{TpRu(L)(NCMe)Ph}$  complexes.

We have demonstrated that a cationic Ru(II) complex supported by a tris(pyrazolyl)alkane ligand  $[(\text{HC}(\text{pz}^5)_3)\text{Ru}(\text{P}(\text{OCH}_2)_3\text{CEt})(\text{NCMe)Ph}][\text{BAR}'_4]$  ( $\text{HC}(\text{pz}^5)_3 = \text{tris}(5\text{-methylpyrazolyl})\text{methane}$ ;  $\text{BAR}'_4 = \text{tetrakis}[3,5\text{-bis}(\text{trifluoromethyl})\text{phenyl}]\text{borate}$ ) successfully increased the TONs (turnover numbers) for an ethylene hydrophenylation over 30-fold compared to  $\text{TpRu}(\text{P}(\text{OCH}_2)_3\text{Et})(\text{NCMe)Ph}$  [21,26]. We found that it was necessary to install methyl groups into the pyrazolyl-alkane ligand to inhibit  $\text{Ru-N}_{\text{pyrazolyl}}$  bond cleavage and intramolecular pyrazolyl C–H activation [45].

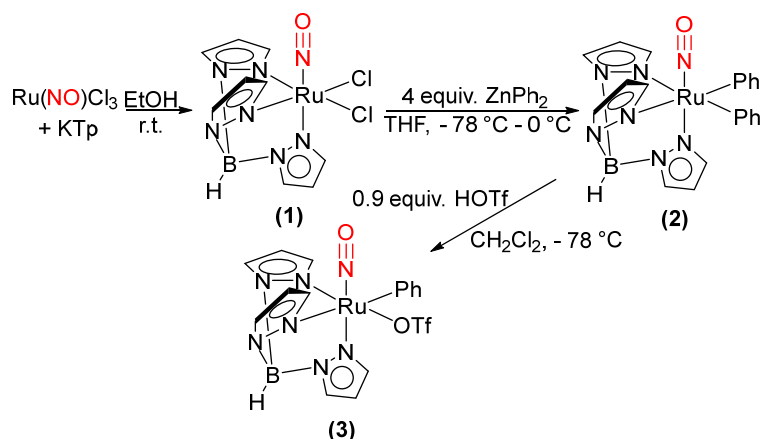
With the success of  $[(\text{HC}(\text{pz}^5)_3)\text{Ru}(\text{P}(\text{OCH}_2)_3\text{CEt})(\text{NCMe)Ph}][\text{BAR}'_4]$  for catalytic hydrophenylation of ethylene, we sought to explore related motifs that might provide reduced electron density at Ru(II). For example, tris(triazolyl)borate ( $\text{Ttz}$ ) ligands have a similar coordination mode to  $\text{Tp}$  and  $\text{HC}(\text{pz}^5)_3$  [46–48], but, compared with the trispyrazolyl borate/methane ligands, the more electronegative nitrogen on the triazole ring may decrease the donor ability of the ligand and lead to a more electron-deficient Ru(II) complex. Moreover, acid additives might bind to a free nitrogen atom of the tris(triazolyl)borate ligand to further reduce its donor ability. Moreover, installation of inductively-electron-

withdrawing groups (e.g., Br) on the pyrazole ring provides another strategy to obtain electron-deficient Ru(II) complexes. Thus, we considered that by replacing the hydrogen atoms on the pyrazole rings of Tp by bromine,  $\text{Tp}^{\text{Br}3}$ , could reduce the donor ability, and allow access to less electron-rich Ru(II) complexes than  $\text{TpRu(L)(NCMe)Ph}$  (Scheme 1).

## 2. Results and Discussion

### 2.1. Attempted Synthesis of Complexes That Provide Access to $[\text{TpRu}(\text{NO})\text{Ph}]^+$

We attempted to synthesize a precursor to  $[\text{TpRu}(\text{NO})(\text{Ph})]^+$  by first preparing  $\text{TpRu}(\text{NO})(\text{OTf})\text{Ph}$  (OTf = trifluoromethanesulfonate) as shown in Scheme 2.  $\text{TpRu}(\text{NO})\text{Cl}_2$  (**1**) was synthesized following a reported procedure with slight modification (see Section 4) [49,50]. The dichloride complex **1** was characterized by IR and  $^1\text{H}$  NMR spectroscopy. The IR spectrum of **1** exhibited an intense absorption at  $1898\text{ cm}^{-1}$ , which is due to NO stretching, and in the  $^1\text{H}$  NMR spectrum of **1**, resonances corresponding to the three Tp-pyrazolyl groups in **1** appear as two sets of signals with a 1:2 integration ratio, which is consistent with the expected mirror plane of symmetry (Figure S1). The complex  $\text{TpRu}(\text{NO})\text{Ph}_2$  (**2**) was synthesized based on a reported procedure [50] from the reaction between **1** and diphenyl zinc in THF with a 54% isolated yield. The diphenyl complex **2** was characterized by IR and  $^1\text{H}$  NMR spectroscopy (Figure S2). The IR spectrum of **2** exhibited an intense band at  $1826\text{ cm}^{-1}$ , indicating the retention of the nitrosyl ligand. The  $\nu_{\text{NO}}$  of **2** is higher energy than that of  $\text{Cp}^*\text{Ru}(\text{NO})\text{Ph}_2$  ( $\text{Cp}^*$  = pentamethylcyclopentadiene;  $1755\text{ cm}^{-1}$ ) [51], demonstrating a smaller degree of  $\pi$ -backdonation from Ru to the  $\text{NO}^+$  ligand by the Ru(II) center supported with Tp [52].



**Scheme 2.** Proposed synthetic route for  $\text{TpRu}(\text{NO})(\text{OTf})\text{Ph}$  (**3**).

Crystals obtained by the slow diffusion of hexanes into a methylene chloride (DCM) solution of **2** were suitable for a single crystal X-ray diffraction study, and the resulting solid-state structure of the complex is shown in Figure 1. However, at room temperature, both solid **2** and a DCM solution of **2** decompose to form a black solid with biphenyl observed as a decomposition product by  $^1\text{H}$  NMR spectroscopy (Scheme 3; Figure S3). Although a detailed reaction pathway for and the final Ru product from the conversion of **2** to form biphenyl was not elucidated, it is possible that an initial reductive elimination of two phenyl groups initiates the decomposition of the Ru complex **2** (Scheme 3). It has been reported by Bergman and coworkers that heating  $\text{Cp}^*\text{Ru}(\text{NO})\text{Ph}_2$  in benzene produces biphenyl and the NO-bridged Ru complexes  $[\text{Cp}^*\text{Ru}(\mu\text{-NO})_2]$  and  $[\text{Cp}^*\text{Ru}(\mu\text{-NO})(\text{Ph})_2]$  (Scheme 3) [51]. With a structurally more bulky, but electronically less donating Tp ligand, complex **2** might be more likely to undergo the reductive elimination reaction than  $\text{Cp}^*\text{Ru}(\text{NO})\text{Ph}_2$  under similar conditions [53].

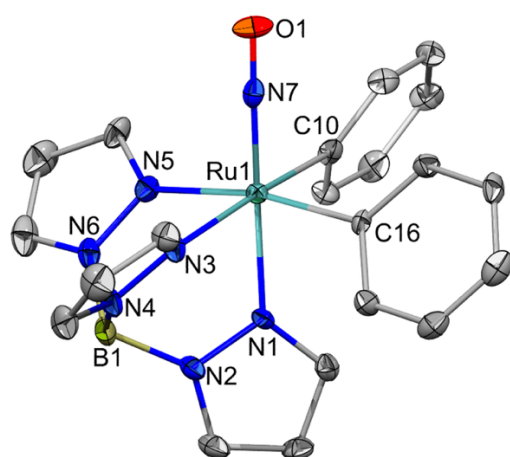
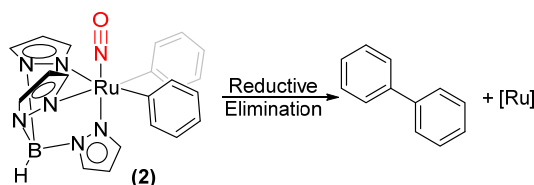
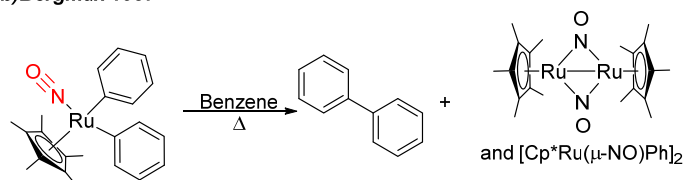


**Figure 1.** ORTEP of  $\text{TpRu}(\text{NO})\text{Ph}_2$  (**2**) with thermal ellipsoids at 50% probability. Hydrogen atoms are omitted for clarity. Only one of the three crystallographically independent but chemically identical molecules in the asymmetric unit is shown. Selected bond lengths ( $\text{\AA}$ ) and bond angles ( $^\circ$ ): Ru(1)-C(10) 2.098(6), Ru(1)-C(16) 2.084(7), Ru(1)-N(7) 1.728(5), N(7)-O(1) 1.151(6), Ru(1)-N(1) 2.119(5), Ru(1)-N(3) 2.174(5), Ru(1)-N(5) 2.167(6); Ru(1)-N(7)-O(1) 177.5(5), C(10)-Ru(1)-C(16) 93.8(2), N(1)-Ru(1)-N(3) 83.70(17), N(1)-Ru(1)-N(5) 81.95(19), N(3)-Ru(1)-N(5) 86.5(2).

**a) This work**



**b) Bergman 1987**



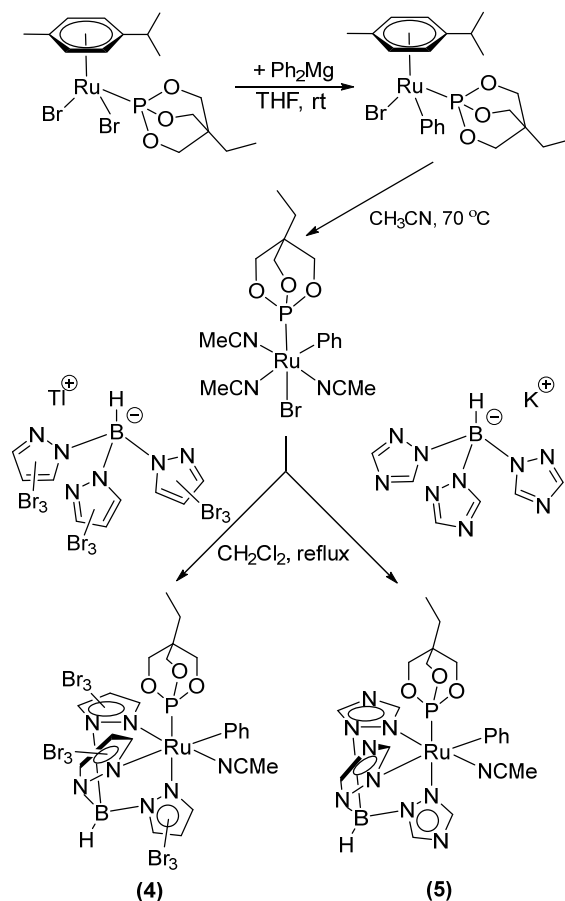
**Scheme 3.** (a) Net reductive elimination of biphenyl from  $\text{TpRu}(\text{NO})\text{Ph}_2$  (**2**) and (b) previously reported biphenyl formation from  $\text{Cp}^*\text{Ru}(\text{NO})\text{Ph}_2$  [51].

Although at room temperature, complex **2** is not stable, it can be stored at  $-40\text{ }^\circ\text{C}$  with no biphenyl formation after at least 2 days. Adding a cold DCM solution of 0.9 equivalents of HOTf into a DCM solution of **2** at  $-78\text{ }^\circ\text{C}$  under inert atmosphere results in a color change from yellow to orange, which likely results from protonation of one of the phenyl groups to form  $\text{TpRu}(\text{NO})(\text{Ph})(\text{OTf})$  (**3**). Complex **3** was isolated as a tan solid by precipitation at low temperature ( $-78\text{ }^\circ\text{C}$ ) with an 80% isolated yield (Scheme 2). The  $^1\text{H}$  NMR spectrum of **3** is consistent with the formation of an asymmetric complex with nine resonances due to the Tp ligand (Figure S4).

Unfortunately, the replacement of a phenyl group with OTf to form complex **3** decreases the stability of the Ru complex. The decomposition of **3** is faster than **2**, and after just a few minutes at room temperature, a pink  $\text{CDCl}_3$  solution of **3** turns dark brown. After 10 min at room temperature, the  $^1\text{H}$  NMR spectrum ( $\text{CDCl}_3$ ) of **3** reveals multiple new resonances due to decomposition (Figure S5). Thus, the instability of complex **3** prevented studies of catalytic olefin hydroarylation.

## 2.2. Ruthenium(II) Complexes Supported by $\text{Tp}^{\text{Br}_3}$ and Ttz Ligands

We synthesized and isolated  $(\text{Tp}^{\text{Br}_3})\text{Ru}(\text{P}(\text{OCH}_2)_3\text{CEt})(\text{NCMe})\text{Ph}$  (**4**) and  $(\text{Ttz})\text{Ru}(\text{P}(\text{OCH}_2)_3\text{CEt})(\text{NCMe})\text{Ph}$  (**5**) (Scheme 4). In order to confirm the successful installation of the phenyl ligand in complex **4**, the reaction of **4** with a Brønsted acid was performed based on the assumption that the phenyl group could be protonated to form free benzene (Scheme S1). Adding one equivalent of trifluoroacetic acid to a  $\text{CDCl}_3$  solution of **4** resulted in the disappearance of all five phenyl resonances (Figure S12), and the concomitant formation of a resonance consistent with the formation of free benzene at 7.35 ppm, which provided further confirmation of the identity of complex **4**.



**Scheme 4.** Synthetic routes for the preparation of  $(\text{Tp}^{\text{Br}_3})\text{Ru}(\text{P}(\text{OCH}_2)_3\text{CEt})(\text{NCMe})\text{Ph}$  (**4**) and  $(\text{Ttz})\text{Ru}(\text{P}(\text{OCH}_2)_3\text{CEt})(\text{NCMe})\text{Ph}$  (**5**).

For  $\text{TpRu}(\text{L})(\text{NCMe})\text{Ph}$  complexes, we observed that rapid rotation of the phenyl ligand on the NMR timescale at room temperature resulted in time averaging of the ortho and meta hydrogen atoms. As a result, the phenyl group in these Ru(II) complexes resonate as three peaks in  $^1\text{H}$  NMR spectrum (Figure 2) [21,26]. In contrast, the room temperature  $^1\text{H}$  NMR spectrum of complex **4** shows restricted rotation of the phenyl ligand where the five hydrogen atoms are not equivalent (i.e., five distinct resonances are observed for the phenyl ligand of **4**). Variable temperature NMR was used to probe the rotation of the Ru–Ph bond in **4**.

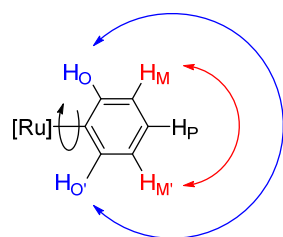


**Figure 2.** Rotation of phenyl group in the TpRu(L)(NCMe)Ph complexes; when the rotation of the Ru-C is rapid, time average of the  $H_O$  and  $H_{O'}$ ,  $H_M$ , and  $H_{M'}$  is observed.

The  $^1\text{H}$  NMR spectra of complex **4** in  $\text{DMSO-}d_6$  were acquired at temperatures between  $20\text{ }^\circ\text{C}$  and  $100\text{ }^\circ\text{C}$  (Figure S13). Four resonances due to the ortho and meta-H atoms are observed at low temperature, but these resonances broaden upon heating, indicating a likely increase in the rate of rotation of the phenyl ligand. At room temperature, the chemical shift difference between the two doublets for the ortho protons in **4** is 870 Hz, and the difference between the triplets for the meta protons is 150 Hz. As the temperature is raised from  $20\text{ }^\circ\text{C}$  to  $100\text{ }^\circ\text{C}$ , the pairs of signals for the ortho and meta protons broaden and average to a broad peak at 6.60 ppm. Based on the slow exchange chemical shift difference and coalescence temperature ( $T_c$ ) of  $80\text{ }^\circ\text{C}$  for the resonances of the ortho protons, a  $\Delta G^\ddagger$  of 14.3 kcal/mol is calculated for the activation barrier for phenyl rotation.

The hydrophenylation of ethylene was attempted using **4** as the catalyst under different ethylene pressures and reaction temperatures. Under all conditions (Table S1), no evidence of catalytic activity was observed. The lack of reactivity is likely due to the large sterically bulky bromine substituents on the Tp ligand, which might prevent olefin coordination.

The  $^1\text{H}$  NMR spectrum of complex **5** is shown in Figure S8. There are six resonances due to the three triazolyl groups, as expected for an asymmetric complex. The cyclic voltammetry of complex **5** shows a reversible Ru(III/II) oxidation at 0.80 V (vs. NHE), which is a +0.25 V shift compared to the previously reported complex TpRu(P(OCH<sub>2</sub>)<sub>3</sub>Cet)(NCMe)Ph (Ru(III/II)  $E_{1/2} = 0.55\text{ V}$ ) [25], indicating the extra N atom on the nitrogen heterocycle ring of complex **5** decreases the donor ability of the poly(triazolyl) ligand compared to Tp, and results in a less electron-rich Ru center. The Ru(III/II) redox potential of 0.80 V for **5** is nearly the same (only 0.02 V more negative) as the Ru(III/II) potential observed for the cationic Ru(II) complex [(HC(pz<sup>5</sup>)<sub>3</sub>Ru(P(OCH<sub>2</sub>)<sub>3</sub>Cet)(NCMe)Ph)][BAR'<sub>4</sub>] [21], which is reported to be the longest lived of our Ru(II) catalysts for ethylene hydrophenylation [21].

Complex **5** was tested as a catalyst for ethylene hydrophenylation reactions. Due to the poor solubility of complex **5** in benzene, catalysis was performed using a low catalyst loading where we observed full dissolution under catalytic conditions. The results of catalysis at different temperatures are shown in Figure 3. At  $75\text{ }^\circ\text{C}$ , the rate of the reaction is slow, and the catalytic turnovers (TOs) reached  $\sim 8$  after 44 h, after which, time catalysis ceased, indicating a likely deactivation of complex **5**. The catalytic performance of **5** increased as the temperature was increased above  $90\text{ }^\circ\text{C}$ , and the initial TOFs (average TOs after 10 h were used to calculate TOFs) of the reaction at  $90\text{ }^\circ\text{C}$ ,  $105\text{ }^\circ\text{C}$ , and  $120\text{ }^\circ\text{C}$  were  $4.5 \times 10^{-4}$ ,  $6.3 \times 10^{-4}$  and  $1.6 \times 10^{-3}\text{ s}^{-1}$ , respectively. However, the high reaction temperatures also led to rapid catalyst deactivation, leading to shortened longevity of 44 h for the reaction at  $90\text{ }^\circ\text{C}$ , 31 h for the reaction at  $105\text{ }^\circ\text{C}$ , and 15 h for the  $120\text{ }^\circ\text{C}$  reaction. Under the conditions studied, optimal catalysis occurs at  $120\text{ }^\circ\text{C}$  to give a total turnover number (TON) of approximately 50 after 20 h, but the majority of the catalysis (TON = 46) is complete after 10 h.

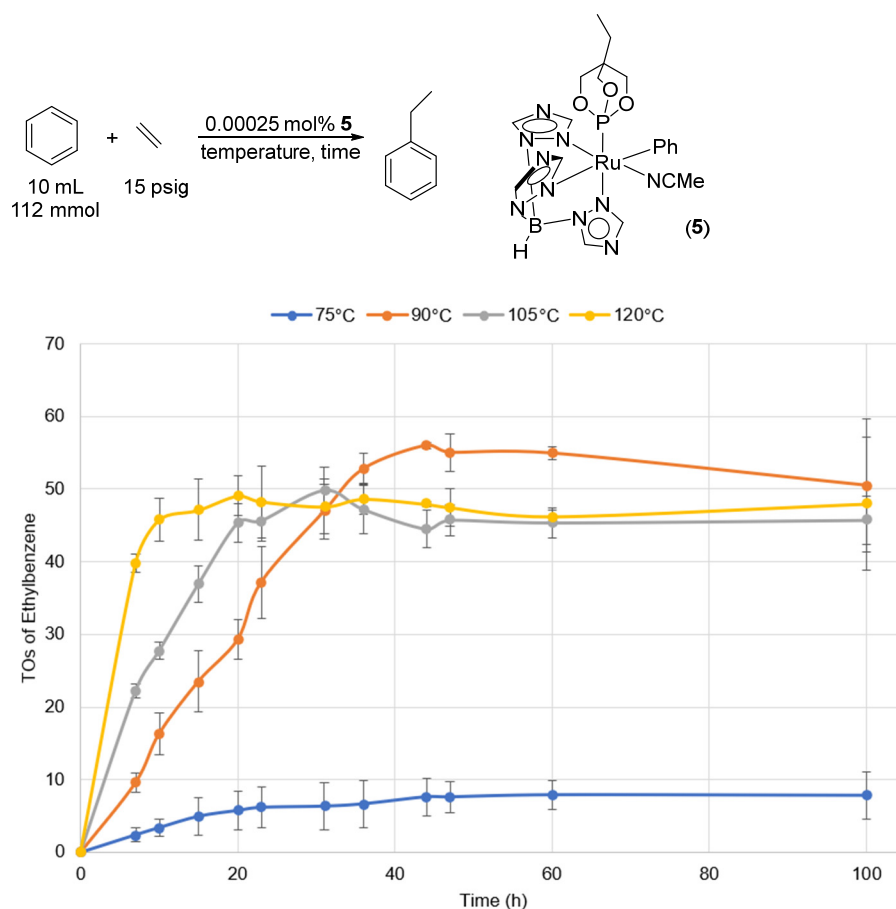


**Figure 3.** Ethylene hydrophenylation catalyzed by  $(\text{Ttz})\text{Ru}(\text{P}(\text{OCH}_2)_3\text{CEt})(\text{NCMe})\text{Ph}$  (**5**) at different temperatures. Conditions: 10 mL benzene solution of 0.00025 mol% complex **5**, 15 psig ethylene; 75, 90, 105, and 120 °C. Error bars represent standard deviations from at least three independent experiments.

Some recent studies have explored the modulation of the  $\sigma$ -donor properties of Ttz via chemical interactions of the *exo*-4-N (Figure 4). Harman, Machan, and co-workers have studied the cyclic voltammetry of  $[\text{TtzMo}(\text{CO})_3]^-$  and  $[\text{TtzW}(\text{CO})_3]^-$  with the presence of Brønsted acid. They observed the protonation of the *exo*-4-N lone pairs of the triazole ring in Ttz ligand, and the single electron oxidation of these species consistent with a proton-coupled electron transfer (PCET) pathway [54]. Work by Papish and co-workers found that ligand protonation of Ttz complexes of first-row transition metals can have a significant effect on the electron density at the metal center [55–60], and that these properties can be used to influence catalytic behavior. Thus, the influence of acid on the catalytic performance of **5** was investigated.

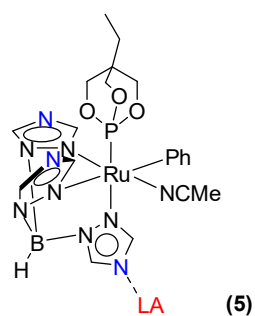


**Figure 4.** The possible interaction between triazole ring and Lewis acid (LA).

Table 1 shows the result of catalytic ethylene hydrophenylation using **5** with the presence of additives. The addition of Brønsted acid (entries 1 and 2) led to decomposition of the catalyst, and no catalytic turnovers were observed. Lewis acids, such as LiNTf<sub>2</sub>, NaNTf<sub>2</sub>, and KNTf<sub>2</sub> (entries 3–5), were shown to positively influence the catalysis, with LiNTf<sub>2</sub> showing an approximate 100% increase compared to catalysis with no additive (TON = 60). This might be explained by the weak coordination of Li<sup>+</sup> with the exo-nitrogen (4-N) on the triazole. Moreover, the coordination of NTf<sub>2</sub> in place of NCMe could play a role in the catalysis, although we did not find any evidence of a Ru–NTf<sub>2</sub> complex. After 6 h of reaction, 147 TON of ethylbenzene with a TOF of  $1.0 \times 10^{-3} \text{ s}^{-1}$  were produced from the reaction of **5** and LiBARF<sub>4</sub>, indicating that Li<sup>+</sup> is responsible for more than a doubled catalytic performance enhancement.

**Table 1.** Effect of additives for ethylene hydrophenylation catalyzed by (Ttz)Ru(P(OCH<sub>2</sub>)<sub>3</sub>CEt)(NCMe)Ph (**5**).

10 mL  
112 mmol

15 psig

0.00025 mol% **5**  
90 °C, 40 hours  
additives

**(5)**

Entry	Additives <sup>a</sup>	TON of Ethylbenzene
1	HNTf <sub>2</sub> <sup>b</sup>	—
2	HBARF <sub>4</sub>	—
3	LiNTf <sub>2</sub>	120(6)
4	NaNTf <sub>2</sub>	91(3)
5	KNTf <sub>2</sub>	54(9)
6	LiBARF <sub>4</sub>	147(12)
7	AlMe <sub>3</sub>	—

Reactions were performed with 0.00025 mol % of complex **5** dissolved in benzene with hexamethylbenzene as an internal standard at 90 °C with 15 psig of ethylene. TONs were determined by GC-FID after 40 h, and the average of three independent experiments. <sup>a</sup> Three equivalents of additive were used in each reaction. <sup>b</sup> NTf<sub>2</sub> = bis(trifluoromethane)sulfonimide.

### 3. Summary and Conclusions

In this work, we have synthesized three electron-deficient Ru(II) catalyst precursors that are supported by Tp or related ligands. These precursors include: (1) a TpRu(II) catalyst with a nitrosyl (formally NO<sup>+</sup>) ligand, which underwent a facile reductive elimination of biphenyl that resulted in catalyst decomposition; (2) a Ru complex supported by Tp<sup>Br3</sup> that exhibited no catalytic reactivity (likely due to its steric hinderance); (3) a Ru complex supported by the Ttz ligand that shows activity as a catalyst for the ethylene hydrophenylation reaction. Compared to our previous Ru(II) catalyst, TpRu(P(OCH<sub>2</sub>)<sub>3</sub>CEt)(NCMe)Ph, (Ttz)Ru(P(OCH<sub>2</sub>)<sub>3</sub>CEt)(NCMe)Ph (**5**) gives a greater than seven-fold increase in TON (147 vs. 20) with the addition of LiBARF<sub>4</sub> as an additive. This is consistent with our previous observation that the decrease of electron density at the Ru(II) center can lead to slower catalyst deactivation.

### 4. Experimental Section

**General Considerations.** Unless otherwise noted, all synthetic procedures were performed under anaerobic conditions in a dinitrogen-filled glovebox, or by using standard Schlenk techniques. Glovebox purity was maintained by periodic nitrogen purges, and was monitored by an oxygen analyzer (O<sub>2</sub> < 15 ppm for all reactions). Tetrahydrofuran (THF) was dried by distillation from sodium/benzophenone. Benzene, *n*-pentane, and CH<sub>2</sub>Cl<sub>2</sub> were purified by passage through a column of activated alumina. Hexanes, CDCl<sub>3</sub>, CD<sub>2</sub>Cl<sub>2</sub>,

and DMSO- $d_6$  were used as received, and stored under a dinitrogen atmosphere over 4 Å molecular sieves, and ethanol was used as received.  $^1\text{H}$  NMR spectra were recorded on a Varian 600, Varian 500 MHz, or a Bruker 600 MHz or 800 MHz spectrometer. All  $^1\text{H}$  spectra are referenced against residual proton signals ( $^1\text{H}$  NMR) of the deuterated solvents.  $^{31}\text{P}\{^1\text{H}\}$  NMR spectra were obtained on a Varian 500 MHz (operating frequency = 201 MHz) or Varian 600 MHz (operating frequency = 243 MHz) spectrometer, and referenced against an external standard of  $\text{H}_3\text{PO}_4$  ( $\delta = 0$ ). GC/MS was performed using a Shimadzu GCMS-QP2010 Plus system with a 30 m  $\times$  0.25 mm capillary column with Rxi-5ms with 0.25  $\mu\text{m}$  film thickness using the electron impact ionization method. GC/FID was performed using a Shimadzu GC-2014 system with a 30 m  $\times$  0.25 mm DB-5ms capillary column with 0.25  $\mu\text{m}$  film thickness. FID response factors for other products were determined in a similar fashion, using authentic standards of products. Electrochemical experiments were performed under a nitrogen atmosphere using a BAS Epsilon potentiostat. Cyclic voltammograms were recorded in  $\text{CH}_3\text{CN}$  using a standard three-electrode cell from 0.4 V to +1.2 V with a glassy carbon working electrode and tetrabutylammonium hexafluorophosphate as the electrolyte. Tetrabutylammonium hexafluorophosphate was recrystallized and dried under dynamic vacuum at 110 °C for 48 h prior to use. All potentials are reported versus NHE (normal hydrogen electrode), using ferrocene as the internal standard. IR spectra were obtained on a Shimadzu IRAffinity-1 Fourier transform infrared spectrometer. All other reagents were used as received from commercial sources. The preparation, isolation, and characterization of  $[(\eta^6\text{-}p\text{-cymene})\text{Ru}(\text{Br})(\mu\text{-Br})_2]$ ,  $\text{Ph}_2\text{Mg}[\text{THF}]_2$ ,  $(\eta^6\text{-}p\text{-cymene})\text{Ru}(\text{P}(\text{OCH}_2)_3\text{CET})(\text{Br})\text{Ph}$ , and  $\text{KTtz}$  (potassium hydridotris(1,2,4-triazol-1-yl)borate) were performed according to the literature procedures [21,26,46,54,61,62]. Elemental analyses were performed by Atlantic Microlab, Inc. X-ray diffraction studies were performed on a Bruker Kappa APEXII Duo system equipped with a fine-focus sealed tube ( $\text{Mo K}\alpha$ ,  $\lambda = 0.71073$  Å) and a graphite monochromator.

**TpRu(NO)Cl<sub>2</sub> (1).** This is a modified procedure based on the literature [50]. A solution of  $\text{Ru}(\text{NO})\text{Cl}_3$  monohydrate (2.37 g, 10 mmol) and two equivalents of  $\text{KTp}$  (5.04 g, 20 mmol) in 150 mL of ethanol was stirred under a dinitrogen atmosphere for two days to yield a dark brownish red mixture. The resulting suspension was filtered through a two-inch pad of Celite, and the filtrate was concentrated to dryness under reduced pressure to get a solid crude product. The resulting solid was dissolved in  $\text{CH}_2\text{Cl}_2$  and purified by column chromatography using a 5-inch plug of silica gel. The pink solution that eluted first is unreacted  $\text{Ru}(\text{NO})\text{Cl}_3$ . The second fraction from the column is  $\text{TpRu}(\text{NO})\text{Cl}_2$ , which was brown. The solvent was then removed under reduced pressure to yield 2.2 g (53%) of complex **1** as a purple solid.  $^1\text{H}$  NMR (600 MHz,  $\text{CDCl}_3$ )  $\delta$  8.15 (dd,  $^3J_{\text{HH}} = 2.3$ ,  $^3J_{\text{HH}} = 0.7$  Hz, 1H, pyrazyl 3-H), 7.91 (d,  $^3J_{\text{HH}} = 2.2$  Hz, 2H, pyrazyl 3-H), 7.80 (dd,  $^3J_{\text{HH}} = 2.5$ ,  $^4J_{\text{HH}} = 0.7$  Hz, 2H, pyrazyl 5-H), 7.59 (dd,  $^3J_{\text{HH}} = 2.4$ ,  $^4J_{\text{HH}} = 0.8$  Hz, 1H, pyrazyl 5-H), 6.43 (t,  $^3J_{\text{HH}} = 2.4$  Hz, 2H, pyrazyl 4-H), 6.27 (t,  $^3J_{\text{HH}} = 2.4$  Hz, 1H, pyrazyl 4-H). IR (KBr):  $\nu_{\text{NO}} = 1898$   $\text{cm}^{-1}$ .

**TpRu(NO)Ph<sub>2</sub> (2).** This is a modified procedure based on the literature [50]. Stirring  $\text{TpRu}(\text{NO})\text{Cl}_2$  (**1**) (415 mg, 1 mmol) in THF under dinitrogen at  $-78$  °C results in a light purple solution. A cold THF solution of four equivalents of  $\text{Ph}_2\text{Zn}$  (880 mg, 4 mmol) was added dropwise to the solution of **1**. After the addition of the  $\text{Ph}_2\text{Zn}$ , the reaction was stirred at  $-78$  °C for an additional 2 h. Then, the reaction mixture was allowed to warm to 0 °C and stirring was maintained for 48 h. The reaction mixture turned brown during this time period. Next, the mixture was filtered through Celite, and the solvent was removed under reduced pressure. The resulting solid was dissolved in  $\text{CH}_2\text{Cl}_2$  and eluted through a plug of silica gel. The brown solution of  $\text{TpRu}(\text{NO})\text{Ph}_2$  (**2**), which eluted after complex **1**, was collected, and the solvent was removed under reduced pressure to give a product with 54% isolated yield (270 mg).  $^1\text{H}$  NMR (600 MHz,  $\text{CDCl}_3$ )  $\delta$  7.78 (dd,  $^3J_{\text{HH}} = 2.4$ ,  $^4J_{\text{HH}} = 0.7$  Hz, 2H, pyrazyl 3-H), 7.64 (dd,  $^3J_{\text{HH}} = 2.2$ ,  $^4J_{\text{HH}} = 0.7$  Hz, 1H, pyrazyl 3-H), 7.39 (dd,  $^3J_{\text{HH}} = 2.0$ ,  $^4J_{\text{HH}} = 0.6$  Hz, 2H, pyrazyl 4-H), 7.20–7.14 (m, 4H, phenyl ortho-H), 7.11 (dd,  $^3J_{\text{HH}} = 2.2$ ,  $^4J_{\text{HH}} = 0.7$  Hz, 1H, pyrazyl 4-H), 7.09–7.03 (m, 4H, phenyl, meta-H), 7.02–6.96

(m, 2H, phenyl para-H), 6.26 (t,  $^3J_{HH} = 2.1$  Hz, 2H, pyrazyl 5-H), 6.10 (t,  $^3J_{HH} = 2.3$  Hz, 1H, pyrazyl 5-H). IR (KBr):  $\nu_{NO} = 1826$  cm $^{-1}$ .

**TpRu(NO)(OTf)Ph (3).** Adding a cold CH<sub>2</sub>Cl<sub>2</sub> solution of 0.9 equivalents of HOTf (27.1 mg, 0.18 mmol) into a CH<sub>2</sub>Cl<sub>2</sub> solution of TpRu(NO)Ph<sub>2</sub> (2) (100 mg, 0.2 mmol) at  $-78$  °C under inert atmosphere resulted in protonation of one of the phenyl groups. The reaction was performed at  $-78$  °C for 2 h, and then allowed to warm to room temperature. A color change of the reaction solution from light brownish red to purple was observed during warming. The solvent was removed under reduced pressure, and the resulting solid was dissolved in DCM and passed through a plug of silica gel using DCM as eluent. The light pink solution was collected, and the solvent was evaporated to obtain TpRu(NO)(OTf)Ph (3) in 80% yield (91.2 mg). <sup>1</sup>H NMR (600 MHz, CDCl<sub>3</sub>)  $\delta$  8.38 (d,  $^3J_{HH} = 2.1$  Hz, 1H, pyrazyl 3-H), 7.89 (dd,  $^3J_{HH} = 2.6$ , 0.7 Hz, 1H, pyrazyl 3-H), 7.76 (dd,  $J = 2.4$ , 0.7 Hz, 1H, pyrazyl 3-H), 7.70 (dd,  $J = 2.4$ , 0.7 Hz, 1H, pyrazyl 4-H), 7.63–7.56 (m, 2H, phenyl ortho-H), 7.48–7.42 (m, 2H, phenyl meta-H), 7.39–7.32 (m, 1H, phenyl para-H), 6.95 (dd,  $^3J_{HH} = 2.7$ ,  $^4J_{HH} = 1.3$  Hz, 1H, pyrazyl 4-H), 6.94 (dd,  $^3J_{HH} = 2.0$ ,  $^4J_{HH} = 1.3$  Hz, 1H, pyrazyl 4-H), 6.39 (t,  $^3J_{HH} = 2.2$  Hz, 1H, pyrazyl 5-H), 6.36 (t,  $^3J_{HH} = 2.4$  Hz, 1H, pyrazyl 5-H), 6.19 (t,  $^3J_{HH} = 2.3$  Hz, 1H, pyrazyl 5-H).

**(Tp<sup>Br3</sup>)Ru(P(OCH<sub>2</sub>)<sub>3</sub>CEt)(NCMe)Ph (4).** The complex ( $\eta^6$ -*p*-cymene)Ru(P(OCH<sub>2</sub>)<sub>3</sub>CEt)(Br)Ph (0.55 g, 1.0 mmol) was dissolved in NCMe (20 mL), added to a pressure tube, and heated for 3.5 h at 70 °C. The reaction was allowed to cool to room temperature. The mixture was filtered through Celite, and the filtrate was concentrated to dryness, yielding the putative complex (NCMe)<sub>3</sub>Ru(P(OCH<sub>2</sub>)<sub>3</sub>CEt)(Br)Ph.<sup>3</sup> The resulting solid was taken up in CH<sub>2</sub>Cl<sub>2</sub> (10 mL) and added to a 50 mL thick-wall glass pressure tube with TITp<sup>Br3</sup> (1.24 g, 1.1 mmol) in DMSO (10 mL). The solution was heated to 70 °C for 15 h, after which, it was cooled to room temperature and filtered through Celite. The volatiles were removed from the filtrate under reduced pressure. Benzene was added, and the mixture was stirred for 10 min. The solution was filtered through Celite, and the filtrate was discarded. The remaining white solid was dissolved in CH<sub>2</sub>Cl<sub>2</sub> and filtered through Celite. The filtrate was concentrated to 2 mL, and hexanes were added to induce precipitation. The colorless precipitate was collected on a fine porosity frit. The solid was washed with pentane and dried in vacuo to yield 1.2 g of tan solid (44%). <sup>1</sup>H NMR (600 MHz, DMSO-*d*<sub>6</sub>)  $\delta$  7.56 (d,  $^3J_{HH} = 7.6$  Hz, 1H, phenyl ortho-H), 6.74 (vt, 1H, phenyl meta-H), 6.59 (tt,  $^3J_{HH} = 7.1$ ,  $^4J_{HH} = 1.3$  Hz, 1H, phenyl para-H), 6.49 (vt, 1H, phenyl meta-H), 6.11 (d,  $^3J_{HH} = 7.8$  Hz, 1H, phenyl ortho-H), 4.18 (d,  $^3J_{PH} = 3.9$  Hz, 6H, P(OCH<sub>2</sub>)<sub>3</sub>CCH<sub>2</sub>CH<sub>3</sub>), 2.40 (s, 3H, NCCH<sub>3</sub>), 1.19 (q,  $^3J_{HH} = 7.6$  Hz, 2H, P(OCH<sub>2</sub>)<sub>3</sub>CCH<sub>2</sub>CH<sub>3</sub>), 0.77 (t,  $^3J_{HH} = 7.7$  Hz, 3H, P(OCH<sub>2</sub>)<sub>3</sub>CCH<sub>2</sub>CH<sub>3</sub>). <sup>31</sup>P{<sup>1</sup>H} NMR (121 MHz, DMSO-*d*<sub>6</sub>)  $\delta$  143.1.

**(Ttz)Ru(P(OCH<sub>2</sub>)<sub>3</sub>CEt)(NCMe)Ph (5).** The complex ( $\eta^6$ -*p*-cymene)Ru(P(OCH<sub>2</sub>)<sub>3</sub>CEt)(Br)Ph (0.55 g, 1.0 mmol) was dissolved in NCMe (20 mL), added to a pressure tube, and heated for 3.5 h at 70 °C. The reaction was allowed to cool to room temperature. The mixture was filtered through Celite, and the filtrate was concentrated to dryness, yielding the putative complex (NCMe)<sub>3</sub>Ru(P(OCH<sub>2</sub>)<sub>3</sub>CEt)(Br)Ph.<sup>3</sup> The resulting solid was taken up in CH<sub>2</sub>Cl<sub>2</sub> (10 mL) and added to a 50 mL thick-wall glass pressure tube with KTtz (0.28 g, 1.1 mmol) in CH<sub>2</sub>Cl<sub>2</sub> (10 mL). The solution was heated to 70 °C for 15 h, after which, it was cooled to room temperature and filtered through Celite. The volatiles were removed from the filtrate under reduced pressure. Benzene was added, and the mixture was stirred for 10 min. The solution was filtered through Celite, and the filtrate was discarded. The remaining white solid was dissolved in CH<sub>2</sub>Cl<sub>2</sub> and filtered through Celite. The filtrate was concentrated to 2 mL, and hexanes were added to induce precipitation. The white precipitate was collected on a fine porosity frit. The solid was washed with pentane and dried in vacuo to yield an off-white solid (262 mg, 43%). <sup>1</sup>H NMR (600 MHz, CDCl<sub>3</sub>)  $\delta$  8.32 (d,  $^3J_{HH} = 2.4$  Hz, 2H, triazole-H), 8.28 (s, 1H, triazole-H), 8.23 (s, 1H, triazole-H), 7.92 (s, 1H, triazole-H), 7.54 (s, 1H, triazole-H), 6.99–6.96 (m, 2H, phenyl-H), 6.89–6.80 (m, 3H, phenyl-H), 4.18 (dt,  $^3J_{PH} = 5.2$ ,  $^4J_{HH} = 2.3$  Hz, 6H, P(OCH<sub>2</sub>)<sub>3</sub>CCH<sub>2</sub>CH<sub>3</sub>), 2.31 (s, 3H, NCCH<sub>3</sub>), 1.19 (q,  $^3J_{HH} = 7.7$  Hz, 2H, P(OCH<sub>2</sub>)<sub>3</sub>CCH<sub>2</sub>CH<sub>3</sub>), 0.82 (t,  $^3J_{HH} = 7.7$  Hz, 3H,

$P(OCH_2)_3CCH_2CH_3$ ).  $^{31}P\{^1H\}$  NMR (121 MHz,  $CD_2Cl_2$ )  $\delta$  133.3. Analyzed and calculated for  $C_{20}H_{26}O_3N_{10}PBRu$ : C, 40.21; H, 4.39; N, 8.04. Found: C, 40.23; H, 4.29; N, 8.17.

**Catalytic Oxidative Hydrophenylation of Ethylene using (Ttz)Ru(P(OCH<sub>2</sub>)<sub>3</sub>CEt)(NCMe)Ph (5).** A representative catalytic reaction is described. A stock solution containing complex 5 (0.023 mmol), hexamethylbenzene (74.5 mg, 0.46 mmol), and benzene (200 mL) was prepared in a volumetric flask. Thick-walled Fisher-Porter reactors were charged with stock solution (10 mL). The vessels were sealed, pressurized with 15 psig of ethylene, and subsequently stirred and heated to the desired temperature (75, 90, 105, and 120 °C) in an oil bath. The reaction was sampled every 2 h. At each time point, the reactors were cooled to room temperature, sampled, recharged with ethylene, and heated. Aliquots of the reaction mixture were analyzed by GC/FID using relative peak areas versus the internal standard.

**Supplementary Materials:** The following supporting information can be downloaded at: <https://www.mdpi.com/article/10.3390/inorganics10060076/s1>, Figure S1:  $^1H$  NMR spectrum of  $TpRu(NO)Cl_2$  (1) in  $CDCl_3$ ; Figure S2:  $^1H$  NMR spectrum of  $TpRu(NO)Ph_2$  (2) in  $CDCl_3$ ; Figure S3:  $^1H$  NMR spectrum of  $TpRu(NO)Ph_2$  (2) in  $CDCl_3$  after 24 hours at room temperature, the production of biphenyl (integrated) is observed; Figure S4:  $^1H$  NMR spectrum of  $TpRu(NO)(OTf)Ph$  (3) in  $CDCl_3$ ; Figure S5:  $^1H$  NMR spectrum of  $TpRu(NO)(OTf)Ph$  (3) in  $CDCl_3$  after 10 minutes at room temperature; Figure S6:  $^1H$  NMR spectrum of  $(Tp^{Br^3})RuP(OCH_2)_3CEt(NCMe)Ph$  (4) in  $DMSO-d_6$ ; Figure S7:  $^{31}P\{^1H\}$  NMR spectrum of  $(Tp^{Br^3})RuP(OCH_2)_3CEt(NCMe)Ph$  (4) in  $DMSO-d_6$ ; Figure S8:  $^1H$  NMR spectrum of  $(Ttz)RuP(OCH_2)_3CEt(NCMe)Ph$  (5) in  $CDCl_3$ ; Figure S9:  $^{31}P\{^1H\}$  NMR spectrum of  $(Ttz)RuP(OCH_2)_3CEt(NCMe)Ph$  (5) in  $CDCl_3$ ; Figure S10: Solid state IR spectrum of  $TpRu(NO)Cl_2$  (1); Figure S11: Solid state IR spectrum of  $TpRu(NO)Ph_2$  (2); Scheme S1. Protonation of  $(Tp^{Br^3})RuP(OCH_2)_3CEt(NCMe)Ph$  (4) by HTFA (trifluoroacetic acid); Figure S12:  $^1H$  NMR spectra of protonation of  $(Tp^{Br^3})RuP(OCH_2)_3CEt(NCMe)Ph$  (4) using HTFA; Figure S13: Variable temperature  $^1H$  NMR spectra of  $(Tp^{Br^3})RuP(OCH_2)_3CEt(NCMe)Ph$  (4) from 20 °C (bottom) to 100 °C (top) in  $DMSO-d_6$ ; Figure S14: CVs of complexes 5 in NCMe; Figure S15: Calibration curve for ethylbenzene quantification on GC-FID; Figure S16: Representative GC-FID chromatogram of a reaction mixture from ethylene hydrophenylation reaction under anaerobic conditions; Table S1: Crystallographic data for  $TpRu(NO)Ph_2$  (2).

**Author Contributions:** X.J. and S.T. performed the synthesis and characterization for the ruthenium complexes; P.J.S. synthesized the Ttz ligand. D.A.D. performed the X-ray data collection and refinement. X.J., W.D.H. and T.B.G. analyzed the data and wrote the paper. T.B.G. administered and supervised the project. All authors have read and agreed to the published version of the manuscript.

**Funding:** This research was funded by the U.S. Department of Energy, Office of Basic Energy Sciences, Chemical Sciences, Geosciences, and Biosciences Division (DE-SC0000776).

**Institutional Review Board Statement:** Not applicable.

**Informed Consent Statement:** Not applicable.

**Data Availability Statement:** CCDC 2170944 contains the supplementary crystallographic data for this paper. These data can be obtained free of charge from The Cambridge Crystallographic Data Centre via [www.ccdc.cam.ac.uk/structures](http://www.ccdc.cam.ac.uk/structures) (accessed on 24 May 2022).

**Acknowledgments:** We thank Pedro Perez (Departamento de Química y Ciencia de los Materiales Universidad de Huelva) for providing a sample of the  $Tp^{Br^3}$  ligand. We thank Ke Zhang for acquiring IR spectra of complexes 1 and 2.

**Conflicts of Interest:** The authors declare no conflict of interest.

## References

1. Garside, M. *Guide to the Business of Chemistry*; American Chemistry Council: Washington, DC, USA, 2019.
2. Gerzeliev, I.M.; Khadzhiev, S.N.; Sakharova, I.E. Ethylbenzene synthesis and benzene transalkylation with diethylbenzenes on zeolite catalysts. *Pet. Chem.* **2011**, *51*, 39–48. [[CrossRef](#)]
3. Čejka, J.; Wichterlová, B. Acid-Catalyzed Synthesis of Mono- and Dialkyl Benzenes over Zeolites: Active Sites, Zeolite Topology, and Reaction Mechanisms. *Catal. Rev.* **2002**, *44*, 375–421. [[CrossRef](#)]

4. Perego, C.; Pollesel, P. Advances in Aromatics Processing Using Zeolite Catalysts. *Adv. Nanoporous Mater.* **2010**, *1*, 97–149.
5. Perego, C.; Ingallina, P. Combining alkylation and transalkylation for alkylaromatic production. *Green Chem.* **2004**, *6*, 274–279. [[CrossRef](#)]
6. Perego, C.; Ingallina, P. Recent advances in the industrial alkylation of aromatics: New catalysts and new processes. *Catal. Today* **2002**, *73*, 3–22. [[CrossRef](#)]
7. Saper, N.I.; Ohgi, A.; Small, D.W.; Semba, K.; Nakao, Y.; Hartwig, J.F. Nickel-catalysed anti-Markovnikov hydroarylation of unactivated alkenes with unactivated arenes facilitated by non-covalent interactions. *Nat. Chem.* **2020**, *12*, 276–283. [[CrossRef](#)]
8. Zhu, W.; Gunnoe, T.B. Advances in Rhodium-Catalyzed Oxidative Arene Alkenylation. *Acc. Chem. Res.* **2020**, *53*, 920–936. [[CrossRef](#)]
9. Zhu, W.; Gunnoe, T.B. Advances in Group 10 Transition-Metal-Catalyzed Arene Alkylation and Alkenylation. *J. Am. Chem. Soc.* **2021**, *143*, 6746–6766. [[CrossRef](#)]
10. Gunnoe, T.B.; Schinski, W.L.; Jia, X.; Zhu, W. Transition-Metal-Catalyzed Arene Alkylation and Alkenylation: Catalytic Processes for the Generation of Chemical Intermediates. *ACS Catal.* **2020**, *10*, 14080–14092. [[CrossRef](#)]
11. Bhalla, G.; Oxgaard, J.; Goddard, W.A.; Periana, R.A. Anti-Markovnikov Hydroarylation of Unactivated Olefins Catalyzed by a Bis-tropolonato Iridium(III) Organometallic Complex. *Organometallics* **2005**, *24*, 3229–3232. [[CrossRef](#)]
12. Periana, R.A.; Liu, X.Y.; Bhalla, G. Novel bis-acac-O,O-Ir(III) catalyst for anti-Markovnikov, hydroarylation of olefins operates by arene CH activation. *Chem. Commun.* **2002**, *24*, 3000–3001. [[CrossRef](#)] [[PubMed](#)]
13. McKeown, B.A.; Foley, N.A.; Lee, J.P.; Gunnoe, T.B. Hydroarylation of Unactivated Olefins Catalyzed by Platinum(II) Complexes. *Organometallics* **2008**, *27*, 4031–4033. [[CrossRef](#)]
14. McKeown, B.A.; Gonzalez, H.E.; Friedfeld, M.R.; Brosnahan, A.M.; Gunnoe, T.B.; Cundari, T.R.; Sabat, M. Platinum(II)-Catalyzed Ethylene Hydrophenylation: Switching Selectivity between Alkyl- and Vinylbenzene Production. *Organometallics* **2013**, *32*, 2857–2865. [[CrossRef](#)]
15. McKeown, B.A.; Gonzalez, H.E.; Friedfeld, M.R.; Gunnoe, T.B.; Cundari, T.R.; Sabat, M. Mechanistic studies of ethylene hydrophenylation catalyzed by bipyridyl Pt(II) complexes. *J. Am. Chem. Soc.* **2011**, *133*, 19131–19152. [[CrossRef](#)] [[PubMed](#)]
16. McKeown, B.A.; Gonzalez, H.E.; Gunnoe, T.B.; Cundari, T.R.; Sabat, M. Pt(II)-Catalyzed Ethylene Hydrophenylation: Influence of Dipyridyl Chelate Ring Size on Catalyst Activity and Longevity. *ACS Catal.* **2013**, *3*, 1165–1171. [[CrossRef](#)]
17. McKeown, B.A.; Gonzalez, H.E.; Michaelos, T.; Gunnoe, T.B.; Cundari, T.R.; Crabtree, R.H.; Sabat, M. Control of Olefin Hydroarylation Catalysis via a Sterically and Electronically Flexible Platinum(II) Catalyst Scaffold. *Organometallics* **2013**, *32*, 3903–3913. [[CrossRef](#)]
18. Clement, M.L.; Grice, K.A.; Luedtke, A.T.; Kaminsky, W.; Goldberg, K.I. Platinum(II) olefin hydroarylation catalysts: Tuning selectivity for the anti-Markovnikov product. *Chem. Eur. J.* **2014**, *20*, 17287–17291. [[CrossRef](#)]
19. Luedtke, A.T.; Goldberg, K.I. Intermolecular hydroarylation of unactivated olefins catalyzed by homogeneous platinum complexes. *Angew. Chem. Int. Ed. Engl.* **2008**, *47*, 7694–7696. [[CrossRef](#)]
20. Andreatta, J.R.; McKeown, B.A.; Gunnoe, T.B. Transition metal catalyzed hydroarylation of olefins using unactivated substrates: Recent developments and challenges. *J. Organomet. Chem.* **2011**, *696*, 305–315. [[CrossRef](#)]
21. Burgess, S.A.; Joslin, E.E.; Gunnoe, T.B.; Cundari, T.R.; Sabat, M.; Myers, W.H. Hydrophenylation of ethylene using a cationic Ru(II) catalyst: Comparison to a neutral Ru(II) catalyst. *Chem. Sci.* **2014**, *5*, 4355–4366. [[CrossRef](#)]
22. Foley, N.A.; Ke, Z.; Gunnoe, T.B.; Cundari, T.R.; Petersen, J.L. Aromatic C–H Activation and Catalytic Hydrophenylation of Ethylene by TpRu{P(OCH<sub>2</sub>)<sub>3</sub>CEt}(NCMe)Ph. *Organometallics* **2008**, *27*, 3007–3017. [[CrossRef](#)]
23. Foley, N.A.; Lail, M.; Gunnoe, T.B.; Cundari, T.R.; Boyle, P.D.; Petersen, J.L. Combined Experimental and Computational Study of TpRu{P(pyr)<sub>3</sub>}(NCMe)Me (pyr = N-pyrrolyl): Inter- and Intramolecular Activation of C–H Bonds and the Impact of Sterics on Catalytic Hydroarylation of Olefins. *Organometallics* **2007**, *26*, 5507–5516. [[CrossRef](#)]
24. Foley, N.A.; Lail, M.; Lee, J.P.; Gunnoe, T.B.; Cundari, T.R.; Petersen, J.L. Comparative reactivity of TpRu(L)(NCMe)Ph (L = CO or PMe<sub>3</sub>): Impact of ancillary ligand l on activation of carbon-hydrogen bonds including catalytic hydroarylation and hydrovinylation/oligomerization of ethylene. *J. Am. Chem. Soc.* **2007**, *129*, 6765–6781. [[CrossRef](#)] [[PubMed](#)]
25. Foley, N.A.; Lee, J.P.; Ke, Z.; Gunnoe, T.B.; Cundari, T.R. Ru(II) catalysts supported by hydridotris(pyrazolyl)borate for the hydroarylation of olefins: Reaction scope, mechanistic studies, and guides for the development of improved catalysts. *Acc. Chem. Res.* **2009**, *42*, 585–597. [[CrossRef](#)] [[PubMed](#)]
26. Joslin, E.E.; McMullin, C.L.; Gunnoe, T.B.; Cundari, T.R.; Sabat, M.; Myers, W.H. Catalytic Hydroarylation of Ethylene Using TpRu(L)(NCMe)Ph (L = 2,6,7-Trioxa-1-phosphabicyclo [2,2,1]heptane): Comparison to TpRu(L')(NCMe)Ph Systems (L' = CO, PMe<sub>3</sub>, P(pyr)<sub>3</sub>, or P(OCH<sub>2</sub>)<sub>3</sub>CEt). *Organometallics* **2012**, *31*, 6851–6860. [[CrossRef](#)]
27. Lail, M.; Arrowood, B.N.; Gunnoe, T.B. Addition of arenes to ethylene and propene catalyzed by ruthenium. *J. Am. Chem. Soc.* **2003**, *125*, 7506–7507. [[CrossRef](#)] [[PubMed](#)]
28. Lail, M.; Bell, C.M.; Conner, D.; Cundari, T.R.; Gunnoe, T.B.; Petersen, J.L. Experimental and Computational Studies of Ruthenium(II)-Catalyzed Addition of Arene C–H Bonds to Olefins. *Organometallics* **2004**, *23*, 5007–5020. [[CrossRef](#)]
29. Matsumoto, T.; Periana, R.A.; Taube, D.J.; Yoshida, H. Direct Synthesis of Styrene by Rhodium-Catalyzed Oxidative Arylation of Ethylene with Benzene. *J. Catal.* **2002**, *206*, 272–280. [[CrossRef](#)]
30. Taube, D.; Periana, R.; Matsumoto, T. Oxidative Coupling of Olefins and Aromatics Using a Rhodium Catalyst and a Copper (I) Redox Agent. Google Patents US6127590A, 3 October 2000.

31. Vaughan, B.A.; Webster-Gardiner, M.S.; Cundari, T.R.; Gunnoe, T.B. Organic chemistry. A rhodium catalyst for single-step styrene production from benzene and ethylene. *Science* **2015**, *348*, 421–424. [[CrossRef](#)]
32. Vaughan, B.A.; Khani, S.K.; Gary, J.B.; Kammert, J.D.; Webster-Gardiner, M.S.; McKeown, B.A.; Davis, R.J.; Cundari, T.R.; Gunnoe, T.B. Mechanistic Studies of Single-Step Styrene Production Using a Rhodium(I) Catalyst. *J. Am. Chem. Soc.* **2017**, *139*, 1485–1498. [[CrossRef](#)]
33. Zhu, W.; Luo, Z.; Chen, J.; Liu, C.; Yang, L.; Dickie, D.A.; Liu, N.; Zhang, S.; Davis, R.J.; Gunnoe, T.B. Mechanistic Studies of Single-Step Styrene Production Catalyzed by Rh Complexes with Diimine Ligands: An Evaluation of the Role of Ligands and Induction Period. *ACS Catal.* **2019**, *9*, 7457–7475. [[CrossRef](#)]
34. Liebov, N.S.; Zhu, W.; Chen, J.; Webster-Gardiner, M.S.; Schinski, W.L.; Gunnoe, T.B. Rhodium-Catalyzed Alkenylation of Toluene Using 1-Pentene: Regioselectivity to Generate Precursors for Bicyclic Compounds. *Organometallics* **2019**, *38*, 3860–3870. [[CrossRef](#)]
35. Jia, X.; Frye, L.I.; Zhu, W.; Gu, S.; Gunnoe, T.B. Synthesis of Stilbenes by Rhodium-Catalyzed Aerobic Alkenylation of Arenes via C–H Activation. *J. Am. Chem. Soc.* **2020**, *142*, 10534–10543. [[CrossRef](#)]
36. Zhu, W.; Gunnoe, T.B. Rhodium-Catalyzed Arene Alkenylation Using Only Dioxide as the Oxidant. *ACS Catal.* **2020**, *10*, 11519–11531. [[CrossRef](#)]
37. Webster-Gardiner, M.S.; Chen, J.; Vaughan, B.A.; McKeown, B.A.; Schinski, W.; Gunnoe, T.B. Catalytic Synthesis of “Super” Linear Alkenyl Arenes Using an Easily Prepared Rh(I) Catalyst. *J. Am. Chem. Soc.* **2017**, *139*, 5474–5480. [[CrossRef](#)]
38. Chen, J.; Nielsen, R.J.; Goddard, W.A., 3rd; McKeown, B.A.; Dickie, D.A.; Gunnoe, T.B. Catalytic Synthesis of Superlinear Alkenyl Arenes Using a Rh(I) Catalyst Supported by a “Capping Arene” Ligand: Access to Aerobic Catalysis. *J. Am. Chem. Soc.* **2018**, *140*, 17007–17018. [[CrossRef](#)] [[PubMed](#)]
39. Luo, Z.; Whitcomb, C.A.; Kaylor, N.; Zhang, Y.; Zhang, S.; Davis, R.J.; Gunnoe, T.B. Oxidative Alkenylation of Arenes Using Supported Rh Materials: Evidence that Active Catalysts are Formed by Rh Leaching. *ChemCatChem* **2021**, *13*, 260–270. [[CrossRef](#)]
40. Jia, X.; Gary, J.B.; Gu, S.; Cundari, T.R.; Gunnoe, T.B. Oxidative Hydrophenylation of Ethylene Using a Cationic Ru(II) Catalyst: Styrene Production with Ethylene as the Oxidant. *Isr. J. Chem.* **2017**, *57*, 1037–1046. [[CrossRef](#)]
41. Weissman, H.; Song, X.; Milstein, D. Ru-catalyzed oxidative coupling of arenes with olefins using O<sub>2</sub>. *J. Am. Chem. Soc.* **2001**, *123*, 337–338. [[CrossRef](#)]
42. Matsumoto, T.; Yoshida, H. Oxidative Arylation of Ethylene with Benzene to Produce Styrene. *Chem. Lett.* **2000**, *29*, 1064–1065. [[CrossRef](#)]
43. Jia, X.; Foley, A.M.; Liu, C.; Vaughan, B.A.; McKeown, B.A.; Zhang, S.; Gunnoe, T.B. Styrene Production from Benzene and Ethylene Catalyzed by Palladium(II): Enhancement of Selectivity toward Styrene via Temperature-dependent Vinyl Ester Consumption. *Organometallics* **2019**, *38*, 3532–3541. [[CrossRef](#)]
44. Bair, J.S.; Schramm, Y.; Sergeev, A.G.; Clot, E.; Eisenstein, O.; Hartwig, J.F. Linear-selective hydroarylation of unactivated terminal and internal olefins with trifluoromethyl-substituted arenes. *J. Am. Chem. Soc.* **2014**, *136*, 13098–13101. [[CrossRef](#)]
45. Joslin, E.E.; Quillian, B.; Gunnoe, T.B.; Cundari, T.R.; Sabat, M.; Myers, W.H. C–H activation of pyrazolyl ligands by Ru(II). *Inorg. Chem.* **2014**, *53*, 6270–6279. [[CrossRef](#)] [[PubMed](#)]
46. Ozkal, E.; Llanes, P.; Bravo, F.; Ferrali, A.; Pericàs, M.A. Fine-Tunable Tris(triazolyl)methane Ligands for Copper(I)-Catalyzed Azide-Alkyne Cycloaddition Reactions. *Adv. Synth. Catal.* **2014**, *356*, 857–869. [[CrossRef](#)]
47. Wang, D.; Etienne, L.; Echeverria, M.; Moya, S.; Astruc, D. A highly active and magnetically recoverable tris(triazolyl)-Cu(I) catalyst for alkyne-azide cycloaddition reactions. *Chem. Eur. J.* **2014**, *20*, 4047–4054. [[CrossRef](#)]
48. Chen, H.; Hou, S.; Tan, Y. An ‘in-water’ halogen-ion compatible “click” catalyst for cucurbituril guest ligation. *Supramol. Chem.* **2016**, *28*, 801–809. [[CrossRef](#)]
49. Arikawa, Y.; Yamaguchi, S.; Haige, R.; Oshiro, E.; Umakoshi, K.; Onishi, M. Methylation of a nitrosylruthenium complex bearing a hydridotris(pyrazolyl)borate ligand. *J. Organomet. Chem.* **2014**, *755*, 12–15. [[CrossRef](#)]
50. Onishi, M. Syntheses and Spectral Properties of New Nitrosyl-[poly(1-pyrazolyl)borato]ruthenium Complexes. *Bull. Chem. Soc. Jpn.* **1991**, *64*, 3039–3045. [[CrossRef](#)]
51. Chang, J.; Bergman, R.G. Reductive elimination leading to transient (*η*-5-C<sub>5</sub>Me<sub>5</sub>) Ru(NO). Trapping, dimerization and oxidative addition reactions of this intermediate and the effect of structural variation on its generation. *J. Am. Chem. Soc.* **1987**, *109*, 4298–4304. [[CrossRef](#)]
52. Tellers, D.M.; Skoog, S.J.; Bergman, R.G.; Gunnoe, T.B.; Harman, W.D. Comparison of the Relative Electron-Donating Abilities of Hydridotris(pyrazolyl)borate and Cyclopentadienyl Ligands: Different Interactions with Different Transition Metals. *Organometallics* **2000**, *19*, 2428–2432. [[CrossRef](#)]
53. Bergman, R.G.; Cundari, T.R.; Gillespie, A.M.; Gunnoe, T.B.; Harman, W.D.; Klinckman, T.R.; Temple, M.D.; White, D.P. Computational Study of Methane Activation by TpRe(CO)<sub>2</sub> and CpRe(CO)<sub>2</sub> with a Stereoelectronic Comparison of Cyclopentadienyl and Scorpionate Ligands. *Organometallics* **2003**, *22*, 2331–2337. [[CrossRef](#)]
54. Heyer, A.J.; Shivokevich, P.J.; Hooe, S.L.; Welch, K.D.; Harman, W.D.; Machan, C.W. Reversible modulation of the redox characteristics of acid-sensitive molybdenum and tungsten scorpionate complexes. *Dalton Trans.* **2018**, *47*, 6323–6332. [[CrossRef](#)] [[PubMed](#)]
55. Bongiovanni, J.L.; Rowe, B.W.; Fadden, P.T.; Taylor, M.T.; Wells, K.R.; Kumar, M.; Papish, E.T.; Yap, G.P.A.; Zeller, M. Synthesis, structural studies and solubility properties of zinc(II), nickel(II) and copper(II) complexes of bulky tris(triazolyl)borate ligands. *Inorg. Chim. Acta* **2010**, *363*, 2163–2170. [[CrossRef](#)]

56. Gardner, S.R.; Papish, E.T.; Monillas, W.H.; Yap, G.P.A. Tris(triazolyl)borate ligands of intermediate steric bulk for the synthesis of biomimetic structures with hydrogen bonding and solubility in hydrophilic solvents. *J. Inorg. Biochem.* **2008**, *102*, 2179–2183. [[CrossRef](#)] [[PubMed](#)]
57. Jernigan, F.E.; Sieracki, N.A.; Taylor, M.T.; Jenkins, A.S.; Engel, S.E.; Rowe, B.W.; Jové, F.A.; Yap, G.P.A.; Papish, E.T.; Ferrence, G.M. Sterically Bulky Tris(triazolyl)borate Ligands as Water-Soluble Analogues of Tris(pyrazolyl)borate. *Inorg. Chem.* **2007**, *46*, 360–362. [[CrossRef](#)] [[PubMed](#)]
58. Kumar, M.; Papish, E.T.; Zeller, M.; Hunter, A.D. Zinc complexes of TtzR, Me with O and S donors reveal differences between Tp and Ttz ligands: Acid stability and binding to H or an additional metal (TtzR, Me = tris(3-R-5-methyl-1,2,4-triazolyl)borate; R = Ph, tBu). *Dalton Trans.* **2011**, *40*, 7517–7533. [[CrossRef](#)]
59. Papish, E.T.; Donahue, T.M.; Wells, K.R.; Yap, G.P.A. How are tris(triazolyl)borate ligands electronically different from tris(pyrazolyl)borate ligands? A study of (TztBu, Me)CuCO [TztBu, Me = tris(3-t-butyl-5-methyl-1,2,4-triazolyl)borate]. *Dalton Trans.* **2008**, *22*, 2923–2925. [[CrossRef](#)]
60. Dixon, N.A.; McQuarters, A.B.; Kraus, J.S.; Soffer, J.B.; Lehnert, N.; Schweitzer-Stenner, R.; Papish, E.T. Dramatic tuning of ligand donor properties in (Ttz)CuCO through remote binding of H<sup>+</sup> (Ttz = hydrotris(triazolyl)borate). *Chem. Commun.* **2013**, *49*, 5571–5573. [[CrossRef](#)]
61. Yakelis, N.A.; Bergman, R.G. Safe Preparation and Purification of Sodium Tetrakis [(3, 5-trifluoromethyl) phenyl] borate (NaBARF24): Reliable and Sensitive Analysis of Water in Solutions of Fluorinated Tetraarylborates. *Organometallics* **2005**, *24*, 3579–3581. [[CrossRef](#)]
62. Lühder, K.; Nehls, D.; Madeja, K. A Simple Method for the Preparation of Dialkyl-Magnesiumorgano or Diarylmagnesiumorgano Compounds. *J. Fur Prakt. Chem.* **1983**, *325*, 1027–1029.